

Overview of Tectonic Subsidence Using the 1D Airy Model in the Dakar Sub-basin Through Backstripping Technique (Senegal, West Africa)

Mohamadou Moustapha THIAM¹, Mouhamadou Afiss DIA¹, Issa NDOYE¹,
Arfang Lamine SOUMARE¹, Adama DIONE¹

¹National Higher School of Mining and Geology,
Cheikh Anta Diop University of Dakar, Senegal.

Corresponding Author: Mohamadou Moustapha THIAM

DOI : <https://doi.org/10.52403/ijrr.20260104>

ABSTRACT

The study investigates the tectonic subsidence history of the MSGBC Basin in Senegal using the 1D Airy backstripping method applied to well GD-1. Results highlight an active post-rift subsidence phase from the Albian to Lower Cenomanian, interrupted by a tecton-thermal uplift event from the Upper Cenomanian to the Lower Conacian. Subsequent slow thermal subsidence reflects lithospheric cooling. The approach provides key insights into the basin's evolution within the Atlantic opening context, though additional well and seismic data are recommended for broader regional understanding.

Keywords: MSGBC basin, backstripping, tectonic subsidence, 1D Airy model, python modelling

INTRODUCTION

The MSGBC Basin, which is the focus of our study, is a vast coastal basin on the West African margin, covering an area of 340,000

km². It is bounded to the east and southeast by the Mauritanides mountain range, and to the south by the Bové Basin in Guinea-Bissau. The MSGBC Basin extends approximately 1,300 km in length from Cap Blanc in Mauritania to Cap Roxo in southern Bissau, Guinea (Figure 1). The sedimentary deposits are primarily marine in origin and date to the Mesozoic-Cenozoic era.

The West African Atlantic margin has long held scientific interest, attracting the curiosity of researchers for decades. Consequently, numerous reconstruction models have been conducted (Pichon & Fox, 1971; Bullard et al., 1965; Vogt, 1973; Hayes & Rabinowitz, 1975, in Latil-Brun, 1987). In this study, we will attempt to examine the evolution of tectonic subsidence within the dynamic context of Atlantic opening and the formation of the MSGBC passive margin basin. For the specific case of passive margin basins, quantitative and geophysical methods have been developed for analyzing crustal evolution (Bond & Kominz, 1984).

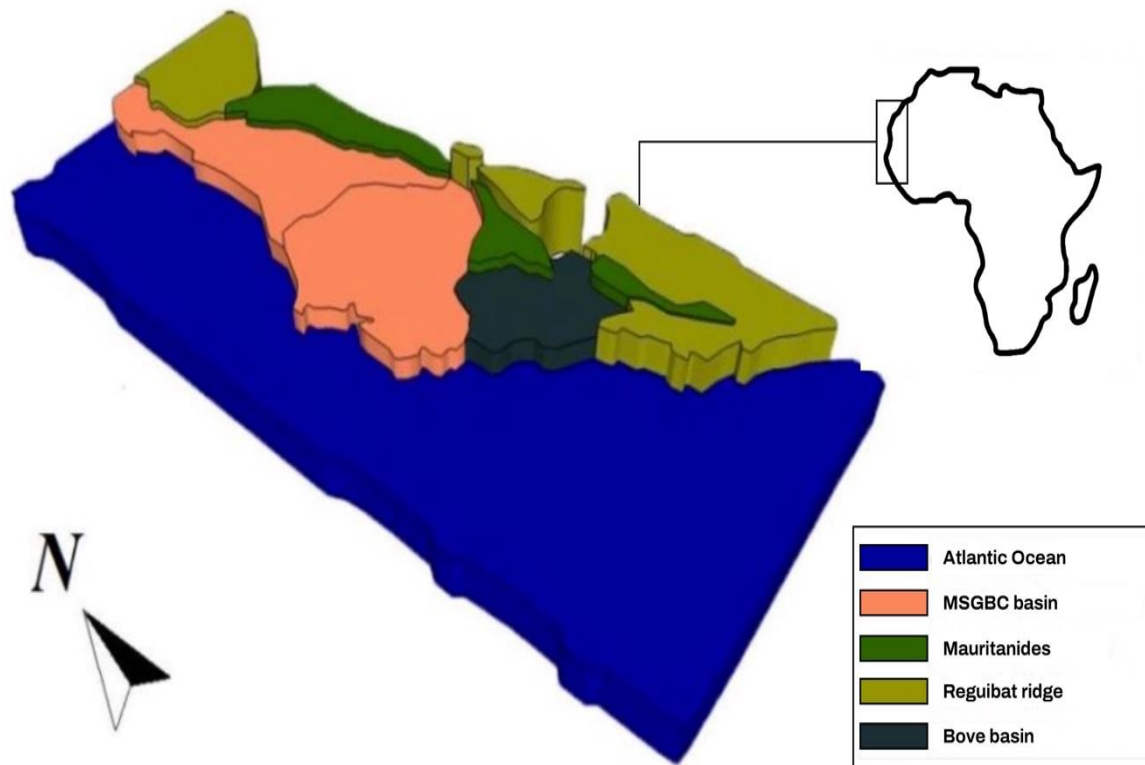


Figure 1. Location map of the MSGBC basin (Thiam, 2016)

The formation of this basin can therefore be summarized into three major phases related to the opening of the Atlantic Ocean (Rochet & Villeneuve, 1987) – see Figure 2:

1. The Pre-rift Phase (Proterozoic – Paleozoic);
2. The Syn-rift Phase (Triassic – Lower Jurassic);
3. The Post-rift Phase (Middle Jurassic to present).

The advantage of analyzing tectonic subsidence through decompaction and backstripping is that the phenomenon can be evaluated without excessive complexity from differences in paleobathymetry, eustasy, compaction, and isostatic effects (Allen & Allen, 2005).

The purpose of backstripping is to analyze the subsidence history of a basin by modeling the reverse processes of progressive sedimentation. In a strict sense, backstripping can be applied to any type of sedimentary basin, and more specifically to extensional basins. In the latter, it is also used to determine the magnitude of lithospheric stretching based on the post-rift subsidence rate (Roberts et al., 1998). The technique consists of first removing sediments from the substrate and then progressively adding them back in succession. During this final phase, it is necessary to account for corrections that must be applied for sediment compaction during burial and, finally, for variations in subsidence resulting from the isostatic response to the sedimentary load.

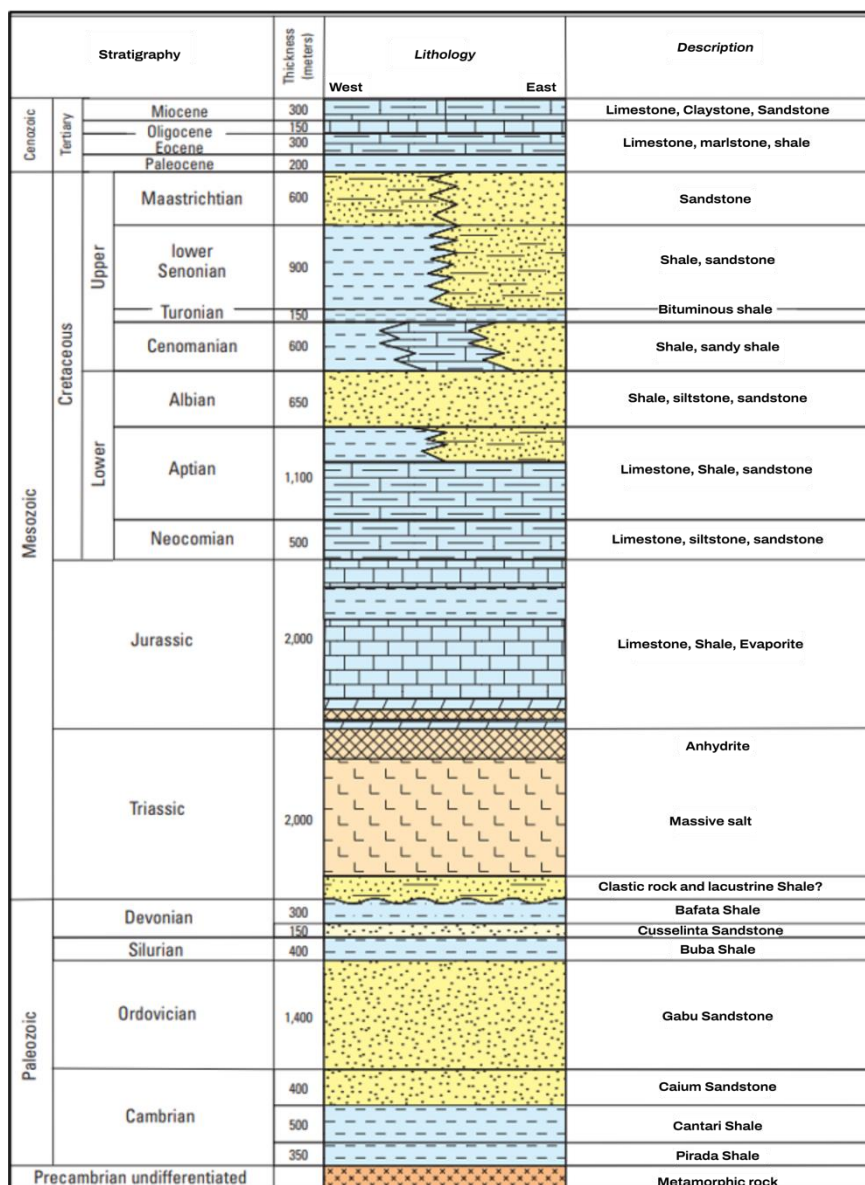


Figure 2. synthetic stratigraphic log of the MSGBC basin (Petrosen, 2024)

MATERIALS & METHODS

1. Backstripping

To study tectonic subsidence in this work, we used data from an oil well, named Gd-1, in order to evaluate the technique and gain insight into the phenomena causing subsidence. The backstripping technique in this study is adapted to the 1D Airy isostatic model. The impact of the sedimentary load on the substrate, depending on burial depth, can be assessed. For a post-rift sequence in an extensional basin context, the 1D Airy model proceeds as follows (Roberts et al., 1998):

- A subsidence curve is constructed by successively removing different layers of the stratigraphic sequence (Figure 3a);
- The remaining stratigraphic layer is then decompacted (Figure 3b);
- Each time a layer is removed, the new depositional surface is considered as the sedimentation depth of the stratigraphic unit (Figure 3c);
- The subsidence curve due to the sedimentary load is corrected based on the subsidence due to the water load.

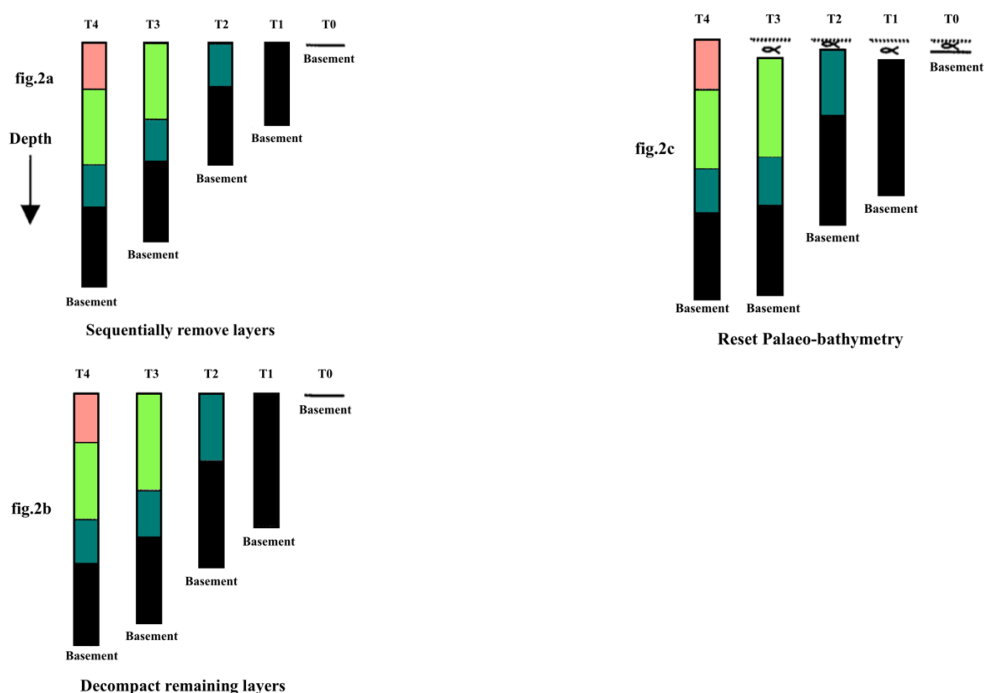


Figure 3. Conceptual steps of the 1D backstripping technique (Roberts et al.; 1998).

It should be noted that another essential assumption of 1D backstripping is that Airy local isostasy is a reliable approximation of the lithosphere's isostatic response to loading. Local isostasy assumes that all loads are compensated solely by vertical movements beneath the load, and that the magnitude of the loads surrounding the sampling point has no effect on its isostatic response (Roberts et al., 1998).

According to Steckler and Watts (1974), tectonic subsidence can be calculated using the following formula:

$$Z = \left[S \left(\frac{\rho_m - \rho_s}{\rho_m - \rho_w} \right) + Wd - \Delta SL \left(\frac{\rho_m}{\rho_m - \rho_w} \right) \right]$$

Z = tectonic subsidence;

S = thickness of decompacted sediments;

ρ_s = apparent average density of sediments;

ρ_m = average density of mantle = 3,40 g/cm³;

ρ_w = density of water;

ΔSL = change in sea level from current level;

Wd = average depth of the water in which the sediments were deposited.

The objective of subsidence models is to explain the spatio-temporal distribution of tectonic subsidence in a sedimentary basin. These models can be grouped into three categories of mechanisms acting separately or simultaneously (Latil-Brun, 1987):

1. Variations in the thermal behavior of the lithosphere, where heat propagates by conduction: an increase in temperature leads to expansion and thus uplift, while a decrease in temperature results in contraction and subsidence;

2. Changes in the pressure-temperature field induce phase transitions, causing variations in the density of the lithosphere. These changes affect the hydrostatic equilibrium at the lithosphere-asthenosphere interface, manifesting as vertical surface movements;

3. Variations in the rheological behavior of the lithosphere (elasticity, plasticity, or viscosity) are considered to predict its evolution when subjected to an overload or extensional stresses.

According to Sleep (1971), the thermal subsidence of passive continental margins exhibited exponential decay growth with a time constant of 50 to 80 Ma. Thus, if no other phenomenon intervened, the

lithosphere that experienced thermal doming would cool and return to its initial position.

2. Python Programming

Within a Python script, we integrated the formula for tectonic subsidence Z and adapted our well data for programming. The first step involves preparing the data from petroleum well reports. This includes tabulating lithostratigraphy, the thicknesses

of stratigraphic units, the density of facies, and fossil information. The latter allowed for the estimation of paleobathymetry (Latil-Brun, 1987).

The parameters to be determined for each stratigraphic unit are: depth, thickness, apparent density of the lithological facies, porosity, and age (Ma). Table 1 shows the input data from the Gd-1 well report used for programming.

Table 1. Input data from the GD-1 well.

<i>depth</i>	<i>Thickness (m)</i>	<i>Density</i>	<i>Porosity</i>	<i>Age (Ma)</i>
0	160	2200	0.45	33.9
160	206	2600	0.25	56
366	600	2200	0.45	66
966	472	2500	0.5	72.1
1438	850	2600	0.6	83.6
2288	735	2700	0.6	93.9
3020	900	2800	0.6	100

We focused on Sclater and Christie (1980) in order to define the constants specific to each lithology.

Table 2. Lithology-specific constants for decompaction (Sclater & Christie, 1980).

<i>Lithology</i>	θ_0	C	ρ_s
Shale	63	0.51	2.72
Sand	49	0.27	2.65
Shaly Sand	56	0.39	2.68
Chalk	70	0.71	2.71

θ_0 = initial porosity of porosity – depth relation (%);

C = coefficient of porosity – depth relation ($\times 10^{-5}$);

ρ_s = average sediment density;

ρ_m = average mantle density (3.3 g/cm^3);

ρ_w = average water density (1.0 g/cm^3).

RESULT AND DISCUSSION

A cross-section from West to East reveals the progressive evolution of subsidence in the basin towards the West, within the context of Atlantic opening (Figure 4).

In Figure 4, the onshore location of the Gd-1 well used in this study is indicated. Subsidence is particularly pronounced in the flexure zone. The total depth reached is 3,920 m in the Albian. The basement was not encountered. A stratigraphic hiatus comprising the uppermost Cenomanian,

Turonian, and the base of the Coniacian is noted at 2,288 m. The wide variety of facies encountered (Figure 5) indicates activities influenced by marine transgression-regression cycles, as evidenced by the presence of foraminifera characteristic of marine environments.

In addition, volcanic activity in the region may have implications for basin subsidence. All data were defined in the Python script (Figure 6).

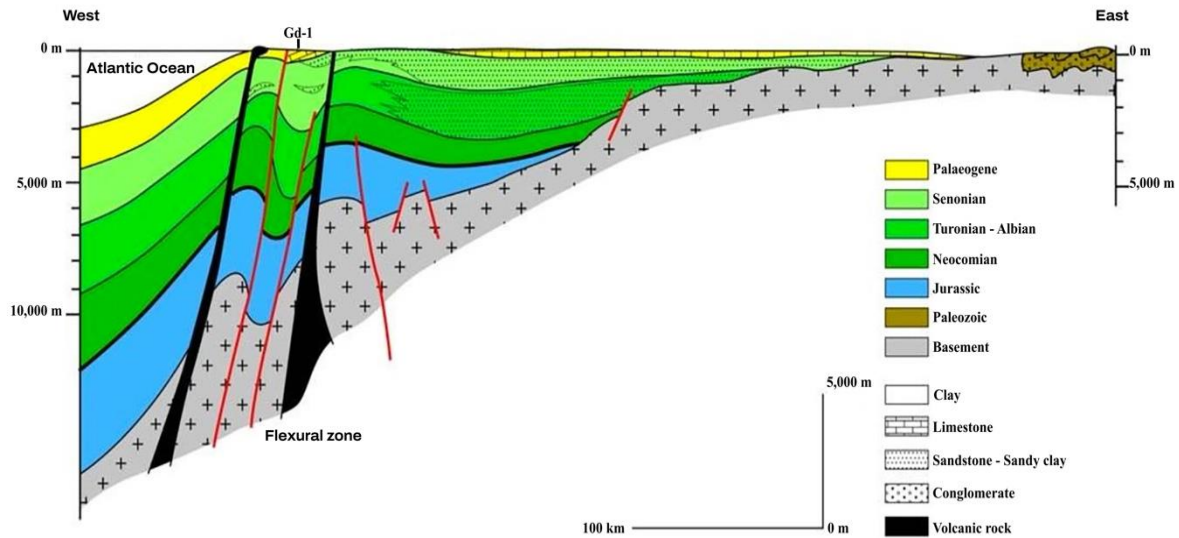


Figure 4. West-East geological cross-section of the Senegalese basin showing the location of the Gd-1 well and the flexure zone (Spengler et al.; 1964; modified).

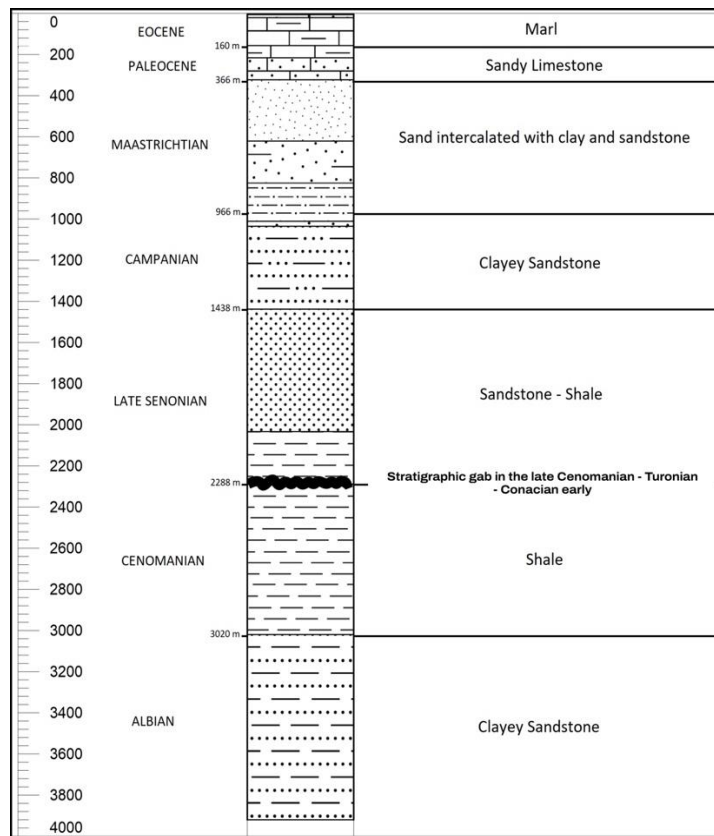


Figure 5. Lithostratigraphic column and main facies encountered in the Gd-1 well.

The programming results are successively presented in Figures 7 and 8.

The compacted curve from the Albian to the Present consistently lies above the decompacted curve, and the difference increases significantly over time. This

indicates strong subsidence and substantial sediment supply.

The well reached the Albian, which partially marks the post-rift phase of the MSGBC Basin. Data related to the Jurassic, representing the Syn-rift phase, were not collected.

```

import numpy as np
import pandas as pd
import matplotlib.pyplot as plt

# Exemple de données de forage
data = pd.DataFrame({
    'age_Ma': [113.0, 100.5, 89.8, 83.6, 72.1, 69, 65, 59, 56, 2.5, 0],
    'thickness_m': [900, 732, 850, 472, 345, 255, 138, 68, 139, 21, 0],
    'density_kg_m3': [2800, 2800, 2700, 2600, 2200, 2200, 2400, 2500, 2600, 2200, 0],
    'initial_porosity': [0.60, 0.60, 0.25, 0.60, 0.60, 0.60, 0.25, 0.25, 0.40, 0.45, 0],
})

# Paramètres de compaction
def porosity(depth, phi0, c):
    return phi0 * np.exp(-c * depth)

def decompacted_thickness(thickness, phi0, c):
    # Approximation par intégration numérique
    depth = np.linspace(0, thickness, 100)
    porosities = porosity(depth, phi0, c)
    return np.trapz(1 / (1 - porosities), depth)

# Calcul de la subsidence tectonique
def backstrip(data, compaction_coeff=0.0005):
    data['decompacted_thickness'] = [
        decompacted_thickness(row['thickness_m'], row['initial_porosity'], compaction_coeff)
        for _, row in data.iterrows()
    ]
    data['tectonic_subsidence'] = data['decompacted_thickness'].cumsum()
    return data

```

Figure 6. Extract of the Python script implemented for tectonic subsidence calculation.

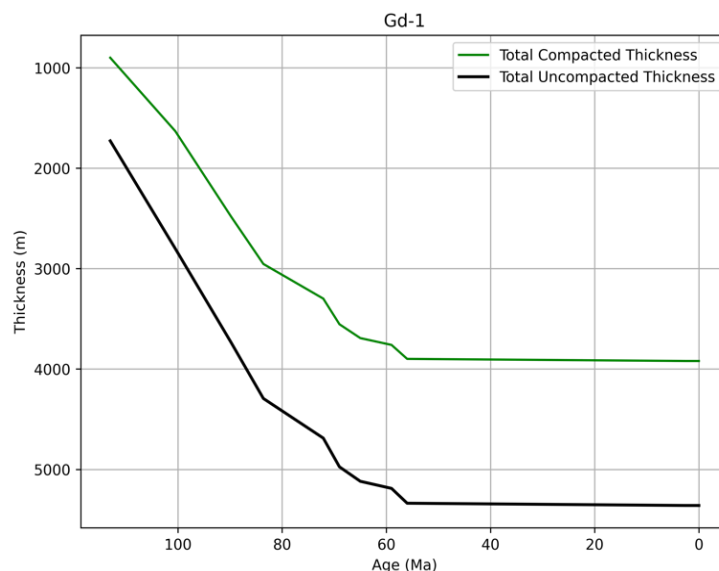


Figure 7. Comparison of compacted versus decompacted thicknesses.

The compacted curve from the Albian to the Present consistently lies above the decompacted curve, and the difference increases significantly over time. This indicates strong subsidence and substantial sediment supply.

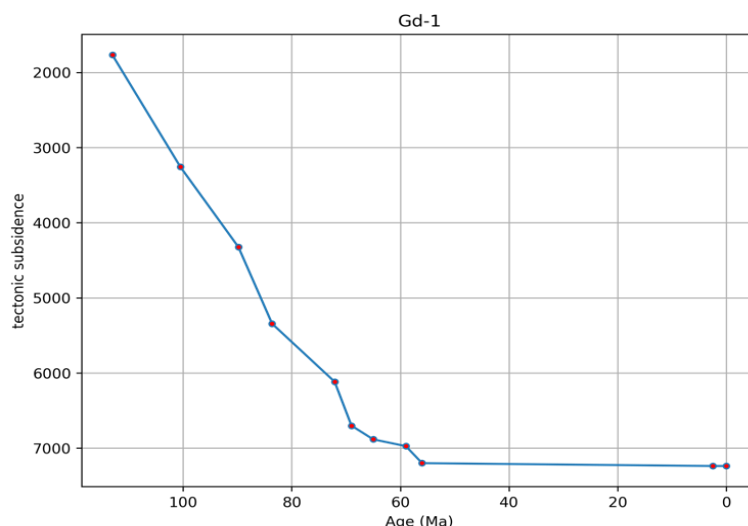


Figure 8. Tectonic subsidence curve.

The general trend of the curve shows a rapidly decreasing phase until approximately 90 Ma, corresponding to the deposition of the top of the Cenomanian, Turonian, and the base of the Coniacian. In the flexure zone and the eastern domain, subsidence begins between 144 Ma and 97.5 Ma, starting during the thermal phase. However, the curves exhibit a rapid phase. Consequently, it is necessary to explain the increasingly younger age towards the East of the initial subsidence phase, as well as the rapid intra-thermal subsidence phases in the western domain (Mpassi, 2004).

The Lower Cenomanian (approximately 105 to 94 Ma) can be considered as the onset of thermal subsidence, with an initially steep subsidence curve that subsequently decreases.

A sedimentary hiatus or erosion is noted from the Upper Cenomanian to the Lower Coniacian (approximately 94 to 86 Ma). The slope of the subsidence curve is steep, indicating a resurgence of tectono-thermal activity. This can be interpreted as tectonic uplift, representing active positive deformation. A volcanic phenomenon, caused by the ascent of hot material, could be responsible for this uplift and the erosion of units from the Upper Cenomanian to the Lower Coniacian.

From 85 to 45 Ma, thermal subsidence resumes but at a slower rate within a context

of marine transgression and increased sediment supply, as illustrated in Figure 7.

From 40 Ma to the Present, the progressive trend of the curve levels off, marking a period of lithospheric cooling.

The age of Tertiary volcanism is placed between the Eocene and the end of the Pliocene (Bellion & Guiraud, 1984). According to Sarr et al., 2000, the occurrence of volcanic activity in the early Lutetian indicates that magmatic activity began earlier in the western part of the basin, coinciding with the first brittle tectonic deformations that started at the end of the Ypresian. These tectonic deformations, which occurred from the base of the Middle Eocene, are actually tectonic uplifts that caused the definitive retreat of the sea over a large part of the basin by the Late Eocene (Mpassi, 2004).

CONCLUSION

From this study, we can identify an active post-rift subsidence phase from the Albian to the base of the Cenomanian. Subsidence was interrupted from the Upper Cenomanian to the Lower Coniacian due to uplift associated with intense tectono-thermal activity. Subsequently, thermal subsidence slowly resumed as the lithosphere cooled, progressively continuing until the Present.

The study of Gd-1 well data using the backstripping method has provided a highly

insightful overview of tectonic subsidence and the probable causes that could explain its evolution.

However, to better refine our understanding of subsidence within the broader context of the MSGBC Basin, it will be necessary to compile additional well and seismic data and compare them across different structural compartments.

Declaration by Authors

Acknowledgement: None

Source of Funding: None

Conflict of Interest: No conflicts of interest declared.

REFERENCES

1. Allen, P. A. & Allen, J. R. (2005). Basin Analysis: Principles and Application to Petroleum Play Assessment (2nd ed.). Blackwell Publishing.
2. Bellion, Y., Guiraud, R. (1984). Le bassin sédimentaire du Sénégal: synthèse de connaissances actuelles. In Plan Minéral de la République du Sénégal. BRGM et DMG, Dakar. Ed, vol 1 p.4-63.
3. Bond, G. C. & Kominz, M. A. (1984). Construction of tectonic subsidence curves for early Paleozoic miogeocline, southern Canadian Rocky Mountains: Implications for subsidence mechanisms, age of breakup, and crustal thinning. Geological Society of America Bulletin, 95 (2), 155-173. Gauvin
4. Bullard, E., Everett, J. E. et Smith, A.G. (1965). The fit of continents around the Atlantic, a symposium on continental drift. Phil. Trans. Roy. Soc. London, v. 258, p. 41-51.
5. Hayes, D. E. et Rabinowitz, R. D. (1975). Mesozoic magnetic lineations and the magnetic quiet zone off Northwest Africa. Earth Planet. Sci. Lett., v. 28, p. 15-19.
6. Latil-Brun, M. V. (1987). Subsidence et évolution thermique du bassin du Sénégal, Comparaison avec la marge divergente homologue est américaine et les marges transformantes de Cote d'Ivoire et des Guyanes. Doctorat és Sciences, Université de Droit, d'Economie et des Sciences d'Aix-Marseille. p.192.
7. Mpassi, D. R. (2004). Contribution à l'étude tectonique de la partie occidentale du bassin sénégalo-mauritanien. Doctorat 3ième cycle de géologie, Université Cheikh Anta Diop, p. 245.
8. Roberts, A. M., Kusznir, N. J., Yielding, G. and Styles, P. (1998). 2D flexural backstripping of extensional basins: the need for a sideways glance. Petroleum Geoscience, Geological Society, London, Vol. 4, pp. 327-338.
9. Sarr, R., Ndiaye, P. M., Niang-Diop, I. et Gueye, M. (2000). Datation par les foraminifères planctoniques d'une activité volcanique, d'âge lutétien, à Toubab Dia Law (Sénégal occidental). Bull. Soc. Géol. France, Paris, 171 (2), 197 – 205.
10. Sclater, J. G. & Christies, P. A. F. (1980). Continental Stretching: an explanation of post mid-Cretaceous subsidence of the Central North Sea Basin. Journal of Geophysical Research, 85, 3711-3739.
11. Sleep, N. H. (1971). Thermal effects of the formation of Atlantic continental margins by continental break up. Geophys. J., v. 24, p.325-350.
12. Spengler, A. de, Castelain, J., Gauvin, J. et Leroy, M. (1966). Le bassin secondaire et tertiaire du Sénégal. In : Symposium New Dehli, 1964, Reyre D. ed., Assoc. Serv. Géol. Afr., Paris, p. 80-94.
13. Steckler, M. S., & Watts, A. B. (1978). Subsidence of the Atlantic-type continental margin off New York. Earth and Planetary Science Letters, 41 (1), 1-13.
14. Thiam, M.M. (2016) Reconstitution tridimensionnelle du bassin sédimentaire sénégalo-mauritanien à l'ouest de la région de Thiès par cartographie numérique. Thèse de doctorat unique, Université de Thiès, Thiès, 126 p.

How to cite this article: Mohamadou Moustapha THIAM, Mouhamadou Afiss DIA, Issa NDOYE, Arfang Lamine SOUMARE, Adama DIONE. Overview of Tectonic Subsidence Using the 1D Airy Model in the Dakar Sub-basin through Backstripping technique (Senegal, West Africa). *International Journal of Research and Review*. 2025; 12(12):33-41.
DOI: <https://doi.org/10.52403/ijrr.20260104>
